

## Solar Hydrogen System for Cooking Applications: Experimental and Numerical Study

Evangelia Topriska<sup>1\*</sup>, Maria Kolokotroni<sup>1</sup>, Zahir Dehouche<sup>1</sup>, Earle Wilson<sup>2</sup>

<sup>1</sup> Brunel University, Uxbridge, United Kingdom

<sup>2</sup> University of Technology, Kingston, Jamaica

\* Corresponding author: [Evangelia.Topriska@brunel.ac.uk](mailto:Evangelia.Topriska@brunel.ac.uk)

### **Abstract**

This paper describes the development of a semi-empirical numerical model for a solar hydrogen system consisting of a Proton Exchange Membrane Electrolyser (PEM) powered by photovoltaic panels to produce hydrogen as fuel for cooking applications, focussing on Jamaica as a suitable case-study. The model was developed in TRNSYS and includes a novel numerical component based on FORTRAN to model the operation of the PEM electrolyser. The numerical component was developed based on operational data from a purpose constructed small-scale experimental rig. The numerical model was calibrated using data from the experimental rig powered by operational data from a photovoltaic panel system in the UK and predicted photovoltaic panel power data from Jamaica. For the test conditions, experiments indicated an electrolysis maximum efficiency of 63.6%. The calibrated model was used to develop a case study analysis for a small community in Jamaica with a daily cooking demand of 39.6 kWh or 1.7 kg of H<sub>2</sub> gas. Simulations indicate that the H<sub>2</sub> production plan is sufficient for the cooking needs of the case-study.

**Keywords:** Solar Hydrogen System, PEM Electrolysis, Photovoltaics, Integrated Renewable Energy, Simulation, Cooking

## 1. Introduction

Over 2.5 billion people depend on firewood, charcoal, agricultural and animal waste to satisfy their energy needs for cooking. Statistics show that death related to indoor air pollution from the use of solid fuels is rated fourth after malnutrition, HIV/ AIDS and lack of clean water [1]. Subsequently, many developing countries have turned to the importation of petroleum based fuels as their main energy source for cooking [2]. The affordability and volatility of oil prices has proven to have a negative impact on the economic and social development of some of these countries [3, 4]. In regions with high solar irradiance one solution would be to use hydrogen as cooking gas produced through photovoltaics powered electrolysis.

Electrolysers are devices that are used to produce hydrogen which can be utilised in a variety of renewable energy systems and industrial [5] and domestic applications [6, 7]. Proton Exchange Membrane electrolysers in particular have been widely facilitated in integrated renewable energy systems as they offer high hydrogen purity, high efficiencies, good partial load response [8, 9] and a compact design with low toxic risk [10, 11]. Producing electrolytic hydrogen with solar energy as a primary source is a sustainable process to provide an energy system with very little environmental cost [12, 13]. This is highlighted in the work of Zini and Tartarini [14] as well as Barbir [15] and Bilgen [16]. Moreover, hydrogen as an energy carrier medium is a promising option that can replace conventional emissions related fuels [17]. Literature review has revealed that most work on renewable hydrogen systems focusses on the produced hydrogen as an energy carrier for electricity generation in fuel cells. Silva et al. [18] describe the application of a stand-alone hybrid solar system to supply a PEM electrolyser in the Brazilian Amazon, where hydrogen is facilitated as energy storage medium

in a fuel cell and battery system that provides electric power. Giatrakos et al. [19] present the design of a hybrid renewable energy/hydrogen power system that can employ PEM electrolyzers to promote energy autonomy in an isolated island. The benefits of a renewable energy powered PEM electrolyser as a part of the energy production scheme in a remote area are also displayed by Bidyut [20], Degiorgis et al. [21], Zoulias and Lympelopoulou [22]. Additionally many technical studies of PV supplied hydrogen production systems have been reported with an aim to model electrolyzers coupled with renewable energy systems by Liu et al. [23], Ghbiri et al. [24], Ursua et al. [25], Joshi et al. [26], Boudries et al. [27] and Ulleberg [28].

Nevertheless, the application of a solar powered electrolyser to produce hydrogen as a cooking fuel has not been reported in the literature. The use of hydrogen as a cooking fuel presents future potential and can contribute towards the improvement of the living and social standards of people, especially those in developing countries [29, 30]. This study focuses on the technical assessment of a system that can produce hydrogen as cooking gas and aims to provide with a model that can be used for the evaluation of its application in various locations when the electrolyser is powered by photovoltaic panels.

The following three sections describe the development of the paper. Section 2 presents the numerical model of the solar hydrogen system, section 3 describes the experimental rig constructed to evaluate the system and provide data for the verification of the numerical model. Section 4 presents a case-study of a large scale simulated application of the system based on the developed numerical model. The application refers to a small Jamaican community of 20 households.

## **2. Description of the Numerical Model Development**

A model that simulates the operation of a solar powered PEM electrolyser system was developed in this study using TRNSYS, which is a transient systems simulation software for the operation of thermal and electrical energy components [31]. Figure 1 shows a screenshot of the developed model applied for the Jamaica case study.

The electrolyser is a compact unit that includes gas and water management systems in addition to the stack. Therefore, its energy use as a unit depends on the total energy requirements of all its components. Hence hydrogen production depends on the fluctuations of the available PV energy in combination with the energy profile of the electrolyser unit, and this is explained in detail in section 2.2. During periods that the available PV electricity is sufficient to power the electrolyser operation, hydrogen is produced and stored in the metal hydride tanks. The system operation for the case study application is based on a monthly supply strategy, with a purpose at the end of each month the metal hydride tanks to be delivered to the households.

Before the simulation of the integrated system the modelling of each component is necessary. This is accomplished through laboratory experimental measurements and also referring to electrochemical models from the literature, as explained below. The basic components of the system that are developed for the purposes of this study are the PEM electrolyser, the controls and gas management and the metal hydride storage components. These act as a combination in the simulation in order to offer the modelling of the compact electrolyser unit.

These novel components are created based on FORTRAN programming and are integrated into the libraries of TRNSYS software. FORTRAN programming language was selected as it is the core programming language of the TRNSYS computational kernel and components.

## **2.1 Proton Exchange Membrane Electrolyser Component**

The PEM electrolyser used in this study is an AC powered unit of one 4-cell stack, manufactured by Proton Onsite [32]. It is rated at 1.2kW and maximum hydrogen production at 600cc/min, with a permissible current of 0-30A, at stack voltage of 6.5-7.5VDC. The characteristic I-V curve of this electrolyser stack is given in Figure 2. The numerical model developed in this study is a semi-empirical model developed from basic electrochemical equations of the electrolysis process and experimental data. The experiments conducted in this part of the study had a purpose to evaluate the electrical performance of the whole electrolyser unit as well as the electrochemical behaviour of the stack itself and derive results regarding the generated flow rates and stack energy use patterns of the electrolyser.

The model is divided in two main submodels. The first is an electrochemical submodel based on experimental analysis of hydrogen generation rates combined with fundamental electrolysis theory resulting in the hydrogen production computation. The experiments examine the hydrogen production rates for pressure set points within the operating range and for a 1 bar interval. The second submodel deals with the stack voltage calculations and is based on thermal semi-empirical methodologies. The combination of these two submodels in a complete model for the PEM electrolyser of this study allows for simulation for any user defined electrolyser size and thus unique stack current, size and temperature.

Finally, a combination of the stack voltage with the input current to the stack allows for the stack energy use calculation.

### 2.1.1. Hydrogen production

In a PEM electrolyser water enters from the anode side and is dissociated into protons, electrons and oxygen with the application of a DC current. Oxygen is released through the anode and protons travel through the proton exchange membrane to the cathode where they are recombined with electrons to form hydrogen [33]. The half reactions characterising the proton exchange membrane electrolysis can be seen in Table 1.

The generated hydrogen amount is calculated by the first law of electrolysis of Faraday, as described in Equation (1):

$$V_{H_2} = \int_0^t \frac{\eta_F \times n_c \times R \times I \times T}{F \times p \times n} dt \quad (1)$$

The Faraday efficiency in general is assumed to be very high, ~99% [8, 10]. Equation (1) has been widely used in reported research to evaluate hydrogen generation rates without taking into consideration any actual losses related to a real system operation.

In a compact hydrogen production system such as the PEM electrolyser used in this study, hydrogen is collected and measured after it passes through gas management modules. The electrolyser includes a drying and purification unit and a hydrogen accumulator that introduce extra inefficiencies in the system. Evaluating the actual effect of these losses on the generated hydrogen flow rates is very important so that the simulation can predict accurate results. These extra losses are evaluated through the experimental process described below.

The effect of the losses and inefficiencies on the generated hydrogen changes according to the generation pressure. Additionally the range of the hydrogen production rates also varies with the production pressure and modelling was based on these flow rates.

The PEM electrolyser used operates for hydrogen production pressures in the range of 3 to 13.8bar, and the amount of the generated hydrogen is different at each pressure set point. The generation rates depend on the set pressure and the stack produces at the adequate rate so as to achieve the necessary pressure at the outlet. Moreover, as the stack presents different operational behaviour at each pressure set point, the energy use is also different. Experiments were conducted and the hydrogen production flow rates, the energy use and temperature of the stack were recorded for pressures between 5 to 13.8bar with a 1bar step, as shown in Figures 3 to 5. The temperature of the electrolyser stack is assumed to be uniform. The flow rates correspond directly to the pressure set point and thus, the higher the pressure the greater the hydrogen generation. Therefore, the stack operates at a more frequent rate to produce the necessary hydrogen and the temperature and energy use increase accordingly.

The pressure at the output was kept constant for each test with back pressure regulation.

The hydrogen generation curve that is developed through polynomial interpolation of the experimental data is given by Equation (2).

$$H_2 = \begin{cases} -4.76 \times 10^{-2} p_{H_2}^3 + 2.23 p_{H_2}^2 + 3.93 p_{H_2} - 2.36 & \text{for } 3 \leq p_{H_2} \leq 13.8 \\ 0 & \text{for } p_{H_2} \leq 3 \text{ or } p_{H_2} \geq 13.8 \end{cases} \quad (2)$$

Where  $H_2$  is the generated hydrogen flow rates in ml/min and  $p_{H_2}$  the pressure of the generated hydrogen in bar.

From Equations (1) and (2) an operation coefficient is derived that is characteristic for the operation at certain pressures within the working range, as given in Table 2. This coefficient takes into consideration the losses caused by the gas management systems as described above and is an index of the actual hydrogen generation in comparison to the maximum theoretical one, which in this case is for  $I=27A$ , 4 cells and 1 stack. The user can model any size of this electrolyser based on this coefficient in order to get the equivalent hydrogen production results. By inputting stack current, stack temperature and number of cells to the model, the model calculates the volumetric flow rates as given in Equation (3). It is observed that the losses are reduced for operation at higher production pressures.

$$V_{H_2Actual} = \int_0^t \frac{\eta_F \times n_c \times CO \times R \times I \times T}{F \times p \times n} dt \quad (3)$$

### 2.1.2. Cell Voltage and Power

The cell voltage of a PEM electrolyser stack has been described and studied by many researchers. Among them are, Larminie and Dicks [34], Dursun et al. [35] and Marangio et al. [36]. The model used in this study for the stack voltage submodel of the PEM electrolyser model is the one suggested by the North Dakota University team [37, 38] and is described by Equation (4).

$$V_{tot} = V_{Nernst} + V_{Activation} + V_{Ohmic} \Rightarrow$$

$$V_{tot} = \left[ V_{rev}^0 + \frac{RT}{nF} \ln\left(\frac{p_{H_2} p_{O_2}^{1/2}}{p_{H_2O}}\right) \right] + \left[ \frac{RT_{an}}{a_{an} F} \operatorname{arcsinh}\left(\frac{j}{2j_{0,an}}\right) + \frac{RT_{cat}}{a_{cat} F} \operatorname{arcsinh}\left(\frac{j}{2j_{0,cat}}\right) \right] + \left[ \left(\frac{\Phi}{\sigma}\right) j \right] \quad (4)$$

Equation (4) shows that the cell voltage is a combination of three different voltages. The first term is the Nernst voltage, where the reversible cell voltage and the partial pressures at the

anode and cathode are taken into account. This is the theoretical voltage that is necessary for the electrolysis without taking into consideration any losses [9, 37]. The second part is called activation overvoltage and it represents the overvoltage that the electrochemical reaction has to overcome in order to initiate. The electrochemical model used to describe this part of the reaction is based on the Butler-Volmer equation. The last term, the ohmic resistance overvoltage is connected to the ohmic losses. The flow of electrons through the current collectors and separator plates faces a resistance, and this is the cause of the ohmic overvoltage. Similarly part of the ohmic resistance is imposed by the conduction of protons through the membrane [37]. The conductivity of the membrane is given by Equation (6) and it depends only on the stack temperature as the membrane is assumed to be fully saturated with water [10].

The reversible cell voltage of the PEM Electrolyser cell is calculated in more detail according to the suggested temperature dependent model of Dale et al. [37] by Equation (5). The standard value of 1.23V for the reversible cell voltage has been widely used by many researchers. Nevertheless, taking into consideration the effect of temperature on the reversible cell voltage enhances the accuracy of the model, as the reversible cell voltage decreases with temperature [37]. The membrane thickness and type, conductivity and exchange current densities that are used in this work are based on the experimental analysis of [37] and [38] on a larger scale PEM electrolyser by the same manufacturer; information regarding these values is not available from the manufacturers. The temperature is input to the model after it was measured experimentally, as shown in Figure 4. For each pressure set point a different maximum stack temperature is recorded as described in section 2.1.1.

$$V_{rev} = 1.5241 - 1.2261 \times 10^{-3} T + 1.1858 \times 10^{-5} T \ln(T) + 5.6692 \times 10^{-7} T^2 \quad (5)$$

$$\sigma = 0.048026 + 8.15178 \times 10^{-4} T + 5.11692 \times 10^{-7} T^2 \quad (6)$$

The power related to the hydrogen production rate of each cell is calculated by Equation (7). The operation coefficient results in the accurate calculation of the average power as the current to the stack varies significantly according to the pressure and consequently the flow rates.

$$P_{H_2} (W) = I \times V_{tot} \times co \quad (7)$$

The energy content of the generated hydrogen is calculated by Equation (8).

$$E_{H_2} (kWh) = \int_0^t H_2 (ml / min) \times 60 (min / h) \times 10^{-6} (m^3 / ml) \times 141.1 (MJ / kg) \times \rho (kg / m^3) \times \frac{1}{3.6} (kWh / MJ) dt \quad (8)$$

The complete TRNSYS component includes the above computational processes and offers the user the possibility to calculate information regarding: (a) hydrogen generation rates, (b) cell and stack voltage, (c) energy use of the stack that corresponds to the generation rates and (d) energy content of the generated hydrogen for HHV (141.1MJ/kg) [39]. The necessary inputs to the model are: (a) stack current, (b) stack temperature, (c) operational pressure, (d) number and size of cells and (e) number of stacks from which the hydrogen flow rates are calculated accordingly.

## 2.2 Electrolyser Controls Component

As mentioned before, the electrolyser is a compact commercial unit with water and gas management features besides the stack where hydrogen is generated. It is important to study the operation and energy use of these auxiliary components as they have an effect on the electrolyser operation. In the case where electrolysers are coupled with renewable energy

systems as a primary source of electricity, the energy use profile of the extra components is imperative to be analysed. Intermittent available energy from renewable sources, such as PV, in combination with variable energy demand of the compact electrolyser unit can result in operation that is subject to stops and start-ups. Therefore, the actual operation of the unit as a combination of the stack operation and its auxiliary components is studied and resulted in the creation of a TRNSYS component regarding the controls of the electrolyser unit.

A palladium purification system that includes a heating element operating at 278°C, a water pump and the electric controls, constitute the extra energy requirements of the electrolyser. The controls components is an empirical model based on the experimental results of the energy use of the electrolyser.

At the beginning of the operation, the electrolyser needs time to reach a generation state and to stabilise. This period is distinct for each pressure set point as it rises with the pressure rise, and constitutes of two sub-periods. The first sub-period refers to the heating of the purification system and the second sub-period to the stack generation. The flow rates correspond directly to the pressure set-point and thus, the higher the pressure the greater the hydrogen generation period is.

The durations of the two phases are:

- 8.5 minutes average for the heating period, at 474W
- 1.55 minutes for the stack generation at 5 bar, at 750W average
- 1.92 minutes for the stack generation at 7 bar, at 750W average
- 2.7 minutes for stack generation at 10 bar, at 750W average
- 3.68 minutes for stack generation at 13.8 bar, at 750W average

The heater works during the start-up of the electrolyser and at certain points during operation that are dependent on the amount of generated hydrogen. Its operation is simulated by a model that introduces the periods where the heater is ON and extra 474W are added to the electrolyser energy demands.

By introducing two components as a combination for the electrolyser operation, the model offers to the users the flexibility to examine sole stack operation or compact electrolyser unit operation. Additionally, it offers the possibility to examine different solutions for the operation of the hydrogen purification system.

### **2.3 Metal Hydride Storage Component**

The traditional hydrogen storage methods are high pressure storage of hydrogen gas and liquid storage. Liquid storage has the drawback of a refrigeration unit that is necessary to maintain hydrogen at cryogenic state, thus adding extra energy costs and complicating the system. High-pressure storage is restricted by the cylinders weight and safety issues. Metal hydrides present higher energy density (6.5 H atoms/cm<sup>3</sup> for MgH<sub>2</sub>) than compressed hydrogen gas (0.99 H atoms/cm<sup>3</sup>) and liquid hydrogen (4.2 H atoms/cm<sup>3</sup>) [40, 41]. In this context the storage of hydrogen in metal hydride form presents a low-pressure safe and promising solution for stationary applications, such as domestic use.

The storage tank used in this study is a metal hydride storage tank developed in the Hydrogen Laboratory of Brunel University. The metal hydride alloy employed is LaNi<sub>5</sub> and 50 gr are contained in the tank. Based on this storage tank, a numerical component was developed that models the absorption and desorption processes and is used as a suggested storage method for

the case study application. The absorbed mass and charging time are described by the basic Equations (9) and (10):

$$H_{2\text{stored}} = \int_0^{\text{ChargingTime}} \text{Flow}\left(\frac{\text{kg}}{\text{min}}\right) dt \quad (9)$$

$$\text{ChargingTime} = \frac{H_{2\text{Max}}}{\text{Flow}\left(\frac{\text{Nm}^3}{\text{min}}\right)} = \frac{150\left(\frac{\text{ml}}{\text{gr}}\right) * 50\text{gr} * 10^{-6}\left(\frac{\text{Nm}^3}{\text{ml}}\right)}{\text{Flow}\left(\frac{\text{Nm}^3}{\text{min}}\right)} = \frac{7.5 * 10^{-3} \text{Nm}^3}{\text{Flow}\left(\frac{\text{Nm}^3}{\text{min}}\right)} \quad (10)$$

The created component can be used to simulate any size of metal hydride storage tank that employs LaNi<sub>5</sub> hydride alloy of 150 (ml/gr) hydrogen absorption ability. The user needs to input the alloy content and the average hydrogen flow input for the suitable pressure (10bar). Additionally, the model offers the possibility to calculate the heat transfer losses of the tank based on the fundamental thermodynamical principals for convective and radiative heat losses, if the user inputs the tank area and heat transfer coefficients for the tank material.

## 2.4 Photovoltaic System

The photovoltaic panels were simulated using standard TRNSYS components for mono-crystalline panels. The component that was used is based on the five-parameter equivalent circuit model by Duffie and Beckman [1991], and reliably extrapolates performance information provided by the manufacturer at standard rating conditions (1,000 W/m<sup>2</sup>, 25°C) to other operating conditions [42]. The panel's current and voltage relation depends on insolation and temperature and is calculated by Equation (11).

$$I = I_L - I_o \left[ \exp\left(\frac{V + I \times R_s}{\alpha}\right) - 1 \right] - \frac{V + I \times R_s}{R_{sh}} \quad (11)$$

Where,  $\alpha = \frac{N_s \times n_f \times k \times T_c}{q}$

The panels are connected to the electrolyser through an inverter that supplies AC voltage at 230V. The losses of the system are computed and the inverter efficiency corresponds to the actual one of the inverter used in the experiments, which has a measured efficiency varying between 86% to 93%, depending on the fraction of power that goes through, and the AC power.

### **3. Experimental study and calibration of TRNSYS model**

A second experimental study of the system was conducted to calibrate the developed numerical model. The experiments had a focus on assessing the operation of the electrolyser and the balance-of-plant when it is coupled to a PV system. The electrolyser operates on a direct coupling with the PV panels and it is important that the model provides accurate results regarding the effect of the available PV power. As explained in section 2.2 when the electrolyser is powered from a renewable energy source, such as the PV panels, it is subject to the availability of the PV yield. Therefore it is subject to shut down and restarts and the generated hydrogen depends on these features. It is thus imperative that the numerical model can accurately respond to the intermittency of the solar energy and predict correctly the hydrogen generation rates.

Two sets of laboratory tests were performed, one for the operation of the electrolyser under weather conditions of the United Kingdom, and one for Jamaica. The operation of the PV panels in the laboratory was emulated through a 1200W programmable DC power supply unit coupled with a 24VDC/230VAC pure sine output power inverter. Python programming was

used and a code was developed that serves the purpose of controlling the DC Power Supply Unit. Digital control signals that correspond to current values in amperes are sent from a Raspberry Pi computer through a 12bit digital to analogue converter. This setup that can be seen in Figure 6 provides an automated operation and offers the flexibility to test for different sets of irradiances in the laboratory.

For the tests, the DC power supply unit is set at 24V constant to match the inverter specifications and the current changes accordingly so that the unit operates as the PV array and the data sent from the Raspberry Pi correspond to current values in Amperes.

### **3.1 Experiments with UK data**

Irradiance data of a 5 minute time interval from Brunel University's weather station and power data from a 1.765kW photovoltaic array are used. The array consists of 4 Sanyo HIT 210W modules of 16.8% maximum efficiency, and 5 Sharp mono-crystalline 185W modules of 14.1% maximum efficiency. The characteristics of the modules are presented in Table 3.

Data selection for the experiments is a critical part of the process. After taking into consideration three years of recorded daily irradiance levels, from 2010 to 2013, data for the first week of June 2013 were selected, as June is the month with the highest irradiance in the UK and the selected set of seven days offer many hours of sunshine and irradiance levels that correspond to the highest PV power in the year. As the application of the system is in Jamaica, the tests should emulate conditions that correspond to high solar irradiance. Additionally, the selected data offer days with clear sky and therefore high irradiance throughout the day as well as days with unstable cloud coverage, where the output of the PV

panels varies significantly. The tests were performed for each day for four different hydrogen production pressures: 5bar, 7bar, 10bar and 13.8bar.

Figures 7 and 8 show the hydrogen production at the four selected pressure points and for two characteristic days of the week selected for the experiments. June 2<sup>nd</sup> is a day with highly variable irradiance due to cloud coverage and June 4<sup>th</sup> is a clear day. The hydrogen production is intermittent during the day with the variable irradiance whereas it is constant during the clear day, for all production pressures. On June 2<sup>nd</sup> the maximum irradiance is 1092 W/m<sup>2</sup> at 12.55 with a PV output of 1165W. It should be noted that the greatest variation in irradiance and thus PV power output during this day is at the same time that irradiance drops by 668W/m<sup>2</sup> and PV power by 450W. June 4<sup>th</sup> has a maximum of 914W/m<sup>2</sup> and peak PV power 1280W.

### **3.2 Experiments with Jamaica data**

For the Jamaica case study a different approach was followed in terms of PV power data. Only weather data of a 15 minute time interval were available for Jamaica, from a weather station installed in the University of Technology in Kingston. The PV power data used in the tests were predicted using the weather data and the standard PV component of TRNSYS for mono-crystalline panels, as described in section 2.4. The PV panels' model used is a TrinaSolar TSM-180DA01, of 180W rated power, forming a 1.5kW array. The module characteristics are presented in Table 3. The panels are oriented towards the south at an inclination angle of 17.9° fixed, an azimuth of 0° and ground reflectance of 0.2. The experiments compared three days in May and three days in December, so as to examine the periods of maximum and minimum irradiance levels. For each day the tests were performed four times, for the selected hydrogen pressures. Figures 9 and 10 present the hydrogen

production trend at four selected pressure points for two days of the experiments; a clear day is shown in Figure 10 for the December tests and a day with variable irradiance in May in Figure 9. It can be seen that the operation of the electrolyser is affected by the unstable irradiance levels. On May 18<sup>th</sup> the maximum irradiance is 1044W/m<sup>2</sup> at 11.15 with a PV output of 1314W. The greatest variation in irradiance and thus PV power output during this day is at 11.30 that irradiance drops by 704W/m<sup>2</sup> and PV power by 994W. December 4<sup>th</sup> has a maximum of 715W/m<sup>2</sup> and peak PV power 1028W at 12.30.

### **3.3 Experimental Results Discussion**

The operation and energy utilisation and efficiency of the system is highly affected by the irradiance levels and subsequently the available PV power output. As explained in section 2.2 the electrolyser is a commercial unit comprised of supplementary components that manage its operation and for that reason it requires a minimum energy supply. This depends mainly on the heater function that is variable, and when it is on it adds approximately 450W to the system. In combination with the stack that requires at maximum 300W a total 750W demand is reached. The integrated system operation is a combination of the available irradiance – PV power output and the energy requirements of the electrolyser. Thus, there are moments that even though the PV output drops below 500W the system keeps operating as the electrolyser energy requirements at that moment consist only of the energy for the stack operation and the valves and pump. In contrast, if at these moments the total system requirements are a combination of the heater and stack operation, the total energy requirements rise to 700-750W and the electrolyser stops producing and goes to idle state.

Hence, operating the electrolyser under this direct connection to the available PV power output sets it subject to stops and start-ups, which in turn affect the efficiency. A comparison

between the efficiency of the electrolyser for the same operational pressure indicates that on the days with stable operation the system performs better. Additionally, the efficiency is affected by the selected pressure set-point and thus the produced hydrogen flow rate. At higher production pressures the efficiency is higher, as the stack operates at a higher rate and higher temperatures, as presented in Table 4. The most efficient operation of the system (5.1kWh for the production of 1Nm<sup>3</sup> of hydrogen) is when the electrolyser is not subject to the intermittency of the power supply, but operates stabilised at the highest hydrogen generation pressure. On the contrary, operating the electrolyser at low operating pressures is always the least efficient way. These results are evaluated in combination with the energy use of the stack in section 2.2. The stack energy demand increases as the operating pressure increases but it is proved that even though operation at highest pressures is more energy demanding the energy content of the produced hydrogen results in more efficient operation. On June 4<sup>th</sup> the total hydrogen production was 27.6Nm<sup>3</sup> at 5bar, 47.3Nm<sup>3</sup> at 7bar, 84.4Nm<sup>3</sup> at 10bar and 137Nm<sup>3</sup> at 13.8bar, as indicated in Table 5. The increase in the hydrogen generation is averagely 70.8% for these pressure set points and is proportionally higher than the increase of the stack energy demand which is averagely 61.7%, as shown in Figure 5. This is indicative of the improved performance of the stack in higher operating pressures. Thus sizing the PV system adequately so that high pressure constant operation is assured is the optimisation strategy for the simulation and the case study application.

### **3.4 Numerical Model calibration/validation**

The experimental results act as a calibration of the developed electrolyser numerical model. Figure 11 shows the hydrogen flow rates for 10bar and operation during the second of June for the UK experimental data. The numerical model is based on the average flow rates for

each specific hydrogen production pressure. Figure 11 shows a good agreement between the actual production trend and the simulated. At the beginning of the operation and at every restart the hydrogen flow rates present a peak which in a few seconds starts to reduce. This is because at the start of the generation process hydrogen is accumulated in the electrolyser until the necessary production pressure levels are achieved. Thus the accumulated gas exits at a high rate and when the pressure is stabilised the flow is stabilised too. Comparison between all the results of the UK and Jamaica experimental sets and the simulation results is performed and the average difference was 6.22% for 5bar, 6.12% for 7bar, 4.46% for 10bar and 3.70% for 13.8bar. The similarity between the experimental and simulation results increases at higher operating pressures as at higher flow rates the effect of the peaks is less prominent. Thus it is concluded that the model can be used with confidence for the simulation of the solar hydrogen system.

### **3.5 Metal Hydride Storage Testing**

The metal hydride storage tank used in these tests consists of LaNi<sub>5</sub> powder form storage alloy as explained in section 2.3. The hydrogen absorption ability of this alloy is 150ml/gr, and thus 7.5Nlt of hydrogen, or 0.67 gr, can be stored in the tank at 10bar. At this pressure with the equivalent flow rate of the electrolyser being averagely 206.17ml/min at 10bar the tank is filled within 28 minutes during the experimental test.

The numerical model filling time is 36 minutes. The difference between the numerical model and the experimental filling times is due to the fact that the hydrogen generation presents flow peaks at the beginning of the operation as explained in section 3.4. In more details, the metal hydride tank is directly connected to the hydrogen outlet through a vacuumed steel pipe

and hydrogen is introduced to the line at 10bar. When the absorption process starts, a pressure drop is observed and the electrolyser stack generates hydrogen at a higher rate to balance the pressure losses. Flow rate peaks of 1100ml/min are observed. As the absorption process develops the flow decreases and eventually stabilises at 206.17ml/min average at 10bar and when the absorption process is nearly completed the flow begins to drop until it is zero. A demonstration of the experimental and the simulation results can be seen in Figure 12.

Here it should be noted that a compressed gas storage component of TRNSYS was also used as an alternative comparative storage method for the simulations. The comparison between the two methods indicates that for the same mass of hydrogen, stored in the metal hydride tank at 10bar, 3.2m<sup>3</sup> of compressed gas storage would be required for one Jamaican household. To provide a reasonable option in terms of size, more than 100bar of pressure would be required, which sets it inappropriate for domestic applications in terms of safety.

## **4. Model Application Discussion**

### **4.1 A case study application in Jamaica**

A scenario has been developed, for an agglomeration of 20 households in a Jamaican neighbourhood. Simulation has been performed in TRNSYS for 8760h in a year, with a simulation timestep of 1min and integration tolerance of 0.001. For each timestep the program computes the PV yield from the inputted weather data and powers the PEM system. According to the developed model, hydrogen generation is calculated, integrated for the defined period and compared to the adequate user demand. Additionally all the features that the model includes and are described in section 2 of this paper are calculated. This

optimisation strategy was followed and the optimal results were achieved with a system size as described in this section.

The daily cooking demand of an average household in Jamaica is 1.98kWh [43]. With a hydrogen cooker efficiency of 60%, the total daily demand for this small community will be satisfied by 1.7kg of hydrogen (component 7 in Figure 1). The system operation is designed so as to maintain the cooking habits of the locals as similar as possible to their usual. LPG cooking stoves are used by 86% of the households in Jamaica [44, 45], and thus a modified hydrogen gas stove introduces no radical changes [46]. Furthermore, more than half of the Jamaican households that use LPG for cooking purchase the cylinders on a monthly basis [47, 48]. The model is therefore designed to include PV panels and a PEM electrolyser sized according to an energy management strategy that satisfies the monthly cooking demand of the chosen community.

The PV system selected is a 100.8kW array of the TrinaSolar modules as described previously (component 4 in Figure 1). The necessary irradiance and temperature features for the PV modules are inputted in the model through the weather data reader component (component 6 in Figure 1). The weather data file used is derived from Meteonorm 7.0 database for Kingston, Jamaica [49].

Two PEM electrolysers are used, with an average production of 1.14Nm<sup>3</sup>/h at 13.8bar, based on the developed numerical model. The optimised sizing of the system is the result of the equilibrium between cost and demand satisfaction. Constant operation of the electrolysers is achieved throughout the daytime and thus the system operates at maximum efficiency.

## **4.2. Case study Simulation Results**

The total cooking demand in one year is 622.05kg and the designed system satisfies this demand by 46kg additional production, and Figure 13 shows that the demand is satisfied at all months. The monthly demand varies between 47.72kg to 52.83kg, depending on the month, and the target is to satisfy each month accordingly. Thus the production, of the preceding month has to satisfy the demand of the following month, as the purpose is to supply the consumers on a monthly basis. Figure 14 shows graphical results from TRNSYS simulation regarding demand satisfaction for one random week in February. During the months where the production surpasses significantly the demand (April to October), the produced hydrogen can be stored as extra buffer in cases of shortages.

## 5. Conclusions

This paper examined the application of a solar powered PEM electrolyser system to produce hydrogen at a large scale as a domestic cooking fuel in developing countries. A numerical model of the system in TRNSYS and a novel component that models the operation of the PEM electrolyser was presented.

The model predicts hydrogen production with a minimum error of 3.7% for the maximum hydrogen production pressure of 13.8bar. The balance-of-plant is important as the electrolyser performs more efficiently at highest hydrogen production pressures and when it is not subject to stops, with a maximum efficiency of 63.6% and specific energy use for the continuous production of hydrogen of 5.1kWh/Nm<sup>3</sup>.

The methodology that was followed for the development of this model can act as an example procedure for modelling commercial compact PEM electrolyser units based on their

generated hydrogen pressure and its effect on the hydrogen generation rates and stack energy use. This technique can prove to be highly useful in cases where electrolyzers are coupled with renewable energy sources and the fluctuations of the available energy in combination with the electrolyser energy requirements can place a constraint in the operation of the system.

Based on the developed model, a large scale case study analysis was performed for a small community in Jamaica. The annual cooking demand of the community was satisfied to 107.4% with a 100.8kW PV array and a 1.14Nm<sup>3</sup>/h, hydrogen generation system with the extra hydrogen to act as backup.

The suggested system has significant capital cost but operational costs are minor, and consist mainly on maintenance. Furthermore, the life span of the system is longer than 20 years and the related emissions are the embedded emissions of the materials, as the solar powered electrolysis process is emission free. Therefore, a government funded solar hydrogen plant is a viable and sustainable solution that can provide free or very low price cooking fuel to developing country communities. Moreover, the currently used cooking fuels (firewood, charcoal and LPG) are related to health and respiratory problems, high emissions and deforestation and are costly and often scarce. Further work of the authors includes the LCA and cost benefit analysis of the system and investigation of the effect of synthetic versus real weather data on applications in other region case studies.

## **7. Acknowledgments**

This project is partly funded by ACP Caribbean & Pacific Research Programme for Sustainable Development of the European Union (EuropeAid/130381/D/ACT/ACP). Thanks

are also due to Hiran Azmin of Brunel University for allowing the use of his experimental rig for the metal hydride tests.

## List of References

- [1] OECD/IEA, “Energy For Cooking in Developing Countries,” OECD/IEA, 2006.
- [2] E. Johnson , “Substituting LP Gas for Wood: Carbon and Deforestation Impacts,” World LP Gas Association, Zurich, 2012.
- [3] O. Lucon, S. Teixeira Coelho and J. Goldemberg, “LPG in Brazil: Lessons and Challenges,” *Energy for Sustainable Development*, vol. 8, no. 3, 2004.
- [4] IEA, “World Energy Outlook,” International Energy Association, Paris, 2006.
- [5] G. Gahleitner, “Hydrogen from Renewable Electricity: An International Review of Power-to-Gas Pilot Plants for Stationary Applications,” *International Journal of Hydrogen Energy*, vol. 2013, no. 38, pp. 2039-2061, 2012.
- [6] G. Zini and P. Tartarini, “Hybrid Systems for Solar Hydrogen: A Selection of Case-Studies,” *International Journal of Hydrogen Energy*, vol. 2009, no. 29, pp. 2585-2595, 2009.
- [7] N. Lympieropoulos and E. Zoulias, *Hydrogen-based Autonomous Power Systems: Techno-economic Analysis of the Integration of Hydrogen in Autonomous Power Systems*, Springer, 2008.
- [8] H. Gorgun, “Dynamic Modelling of a Proton Exchange Membrane Electrolyser,” *International Journal of Hydrogen Energy*, vol. 31, no. 2006, pp. 29-38, 2006.
- [9] M. Carmo, D. L. Fritz, J. Mergel and D. Stolten, “A Comprehensive Review on PEM Water Electrolysis,” *International Journal of Hydrogen Energy*, vol. 38, pp. 4901-4934, 2013.
- [10] R. Garcia-Valverde, N. Espinosa and A. Urbina, “Simple PEM Water Electrolyser Model and Experimental Validation,” *International Journal of Hydrogen Energy*, vol. 37, no. 2012, pp. 1927-1938, 2011.
- [11] S. Siracusano, V. Baglio, N. Briguglio, G. Brunaccini, G. Di Blasi, A. Stassi, R. Ornelas, E. Trifoni, V. Antonucci and A. S. Arico, “An electrochemical Study of a PEM Stack for Water Electrolysis,” *International Journal of Hydrogen Energy*, vol. 37, no. 2012, pp. 1939-1946, 2011.
- [12] J. Nowotny and N. Veziroglou, “Impact of Hydrogen on the Environment,” *International Journal of Hydrogen Energy*, pp. 13218-13224, 2011.
- [13] V. A. Goltsov and N. T. Veziroglou, “From Hydrogen Economy to Hydrogen Civilization,” *International Journal of Hydrogen Energy*, vol. 26, no. 2001, pp. 909-915, 2001.
- [14] G. Zini and P. Tartarini, *Solar Hydrogen Energy Systems*, Milano: Springer, 2012.
- [15] F. Barbir, “PEM Electrolysis for Production of Hydrogen from Renewable Energy Sources,” *Solar Energy*, vol. 78, no. 2005, pp. 661-669, 2005.

- [16] E. Bilgen, “Solar Hydrogen for Photovoltaic-Electrolyser Systems,” *Energy Conversion and Management*, no. 42, pp. 1047-1057, 2001.
- [17] N. T. Veziroglou and S. Sahin, “21st Century's Energy: Hydrogen Energy System,” *Energy Conversion and Management*, vol. 49, no. 2008, pp. 1820-1831, 2008.
- [18] S. B. Silva, M. M. Severino and M. de Oliveira, “A Stand-Alone Hybrid Photovoltaic, Fuel Cell and Battery System: A Case Study of Tocantins, Brazil,” *Renewable Energy*, vol. 57, no. 2013, pp. 384-389, 2013.
- [19] G. P. Giatrakos, T. D. Tsoutsos, P. G. Mouchtaropoulos, G. D. Naxakis and G. Stavrakakis, “Sustainable Energy Planning based on a Stand-Alone Hybrid Renewable Energy/Hydrogen Power System: Application in Karpathos Island, Greece,” *Renewable Energy*, vol. 34, no. 2009, pp. 2562-2570, 2009.
- [20] P. Bidyut, *Direct Coupling of the Photovoltaic Array and PEM Electrolyser in Solar Hydrogen Systems for Remote Area Power Supply*, Melbourne: RMIT University, 2009.
- [21] L. Degiorgis, M. Santarelli and M. Cali, “Hydrogen from Renewable Energy: A pilot plant for thermal production and mobility,” *Journal of Power Sources*, p. 10, 2007.
- [22] E. Zoulias and N. Lymperopoulos, “Techno-economic Analysis of the Integration of Hydrogen Energy Technologies in Renewable Energy based Stand Alone Power Systems,” *Renewable Energy*, vol. 32, pp. 680-696, 2007.
- [23] Z. Liu, Z. Qiu, Y. Luo, M. Zongqiang and C. Wang, “Operation of First Solar-Hydrogen System in China,” *International Journal of Hydrogen Energy*, vol. 35, no. 2010, pp. 2762-2766, 2009.
- [24] D. Ghbiri, A. Khelifa, S. Diaf and M. Belhamel, “Study of Hydrogen Production System by using PV Solar Energy and PEM Electrolyser in Algeria,” *International Journal of Hydrogen Energy*, no. 2912, pp. 1-11, 2012.
- [25] A. Ursua, I. San Martin, E. L. Barrios and P. Sanchis, “Stand-alone operation of an Alkaline Water Electrolyser fed by Wind and Photovoltaic Systems,” *International Journal of Hydrogen Energy*, vol. 38, no. 2013, pp. 14952-14967, 2013.
- [26] A. S. Joshi, I. Dincer and B. V. Reddy, “Solar Hydrogen Production: A comparative Performance Assessment,” *International Journal of Hydrogen Energy*, vol. 36, no. 2011, pp. 11246-11257, 2011.
- [27] R. Boudries, A. Khellaf, A. Aliane, L. Ihaddaden and F. Khida, “PV System Design for Powering an Industrial Unit for Hydrogen Production,” *International Journal of Hydrogen Energy*, vol. 39, no. 2014, pp. 15188-15195, 2014.
- [28] O. Ulleberg, “The Importance of Control Strategies in PV-Hydrogen Systems,” *Solar Energy*, vol. 76, no. 2004, pp. 323-329, 2004.
- [29] UN, “Millennium Project,” UN, 2006. [Online]. Available: <http://www.unmillenniumproject.org/goals/gti.htm#goal1>. [Accessed October 2014].
- [30] World Health Organisation, “Fuel For Life - Household Energy and Health,” WHO , 2006. [Online]. Available: <http://www.who.int/indoorair/publications/fuelforlife.pdf>. [Accessed October 2014].
- [31] The University of Wisconsin, “TRNSYS 17,” February 2013. [Online]. Available: <http://sel.me.wisc.edu/trnsys/features/features.html>. [Accessed September 2014].
- [32] P. OnSite, “Proton OnSite,” 2014. [Online]. Available: <http://protononsite.com>.

[Accessed September 2014].

- [33] IEA, “Hydrogen Production and Storage,” International Energy Agency, Paris, 2006.
- [34] J. Larminie and A. Dicks, *Fuel Cell Systems Explained*, Chichester, England: John Wiley & Sons, 2003.
- [35] E. Dursun, B. Acarkan and O. Kilic, “Modeling of Hydrogen Production with a Stand-Alone Renewable Hybrid Power System,” *International Journal of Hydrogen Energy*, vol. 37, no. 2012, pp. 3098-3107, 2012.
- [36] F. Marangio, M. Santarelli and M. Cali, “Theoretical Model and Experimental Analysis of a High Pressure PEM Water Electrolyser for Hydrogen Production,” *International Journal of Hydrogen Energy*, vol. 34, no. 2009, pp. 1143-1158, 2009.
- [37] N. Dale, M. Mann and H. Salehfar, “Semiempirical model based on thermodynamic principles for determining 6kW proton exchange membrane electrolyser stack characteristics,” *Journal of Power Sources*, p. 6, 2008.
- [38] C. Y. Biaku, N. V. Dale, M. D. Mann, H. Salehfar, A. J. Peters and T. Han, “A semiempirical Study of the Temperature Dependence of the Anode Charge Transfer Coefficient of a 6kW PEM Electrolyser,” *International Journal of Hydrogen Energy*, vol. 33, no. 2008, pp. 4247-4254, 2008.
- [39] R. B. Gupta, *Hydrogen Fuel-Production, Transport and Storage*, Boca Raton, Florida: Taylor & Francis Group LLC, 2009.
- [40] B. Sakintuna, F. Lamari-Darkrim and M. Hirscher, “Metal Hydride Materials for Solid Hydrogen Storage: A Review,” *International Journal of Hydrogen Energy*, pp. 1121-1140, 2007.
- [41] Z. Dehouche, M. Savard, F. Laurencelle and J. Goyette, “Ti–V–Mn Based Alloys for Hydrogen Compression System,” *Journal of Alloys and Compounds*, vol. 400, no. 2005, pp. 276-280, 2005.
- [42] TRNSYS 17, “Mathematical Reference,” Solar Energy Laboratory, University of Wisconsin, Madison, 2012.
- [43] The Planning Institute and the Statistical Institute of Jamaica, “Residential Consumer End Use Survey,” The Planning Institute and the Statistical Institute of Jamaica, Kingston, 2007.
- [44] Ministry of Energy and Mining, “Oil Import Statistics,” Ministry of Energy and Mining, Jamaica, Kingston, 2009.
- [45] Ministry of Energy and Mining, Jamaica, “National Renewable Energy Policy, 2009-2030,” Ministry of Energy and Mining, Jamaica, Kingston, 2010.
- [46] University of Technology, Jamaica, “Sustainable Hydrogen Cooking Gas,” 2014. [Online]. Available: <http://www.solarhydrogen.utechsapna.com/Media/Brochure%205.pdf>. [Accessed October 2014].
- [47] “Global Alliance for Clean Cookstoves,” United Nations Foundations, 2014. [Online]. Available: <http://www.cleancookstoves.org/resources/data-and-statistics/>. [Accessed October 2014].
- [48] The World Bank, “Jamaica Development Indicators, Latin America and Caribbean, (developing only),” 2014. [Online]. Available:

<http://data.worldbank.org/country/jamaica?display=default>. [Accessed May 2014].

[49] Meteonorm, “Meteonorm Global Meteorological database,” May 2014. [Online]. Available: [http://meteonorm.com/images/uploads/downloads/mn71\\_software.pdf](http://meteonorm.com/images/uploads/downloads/mn71_software.pdf). [Accessed June 2014].

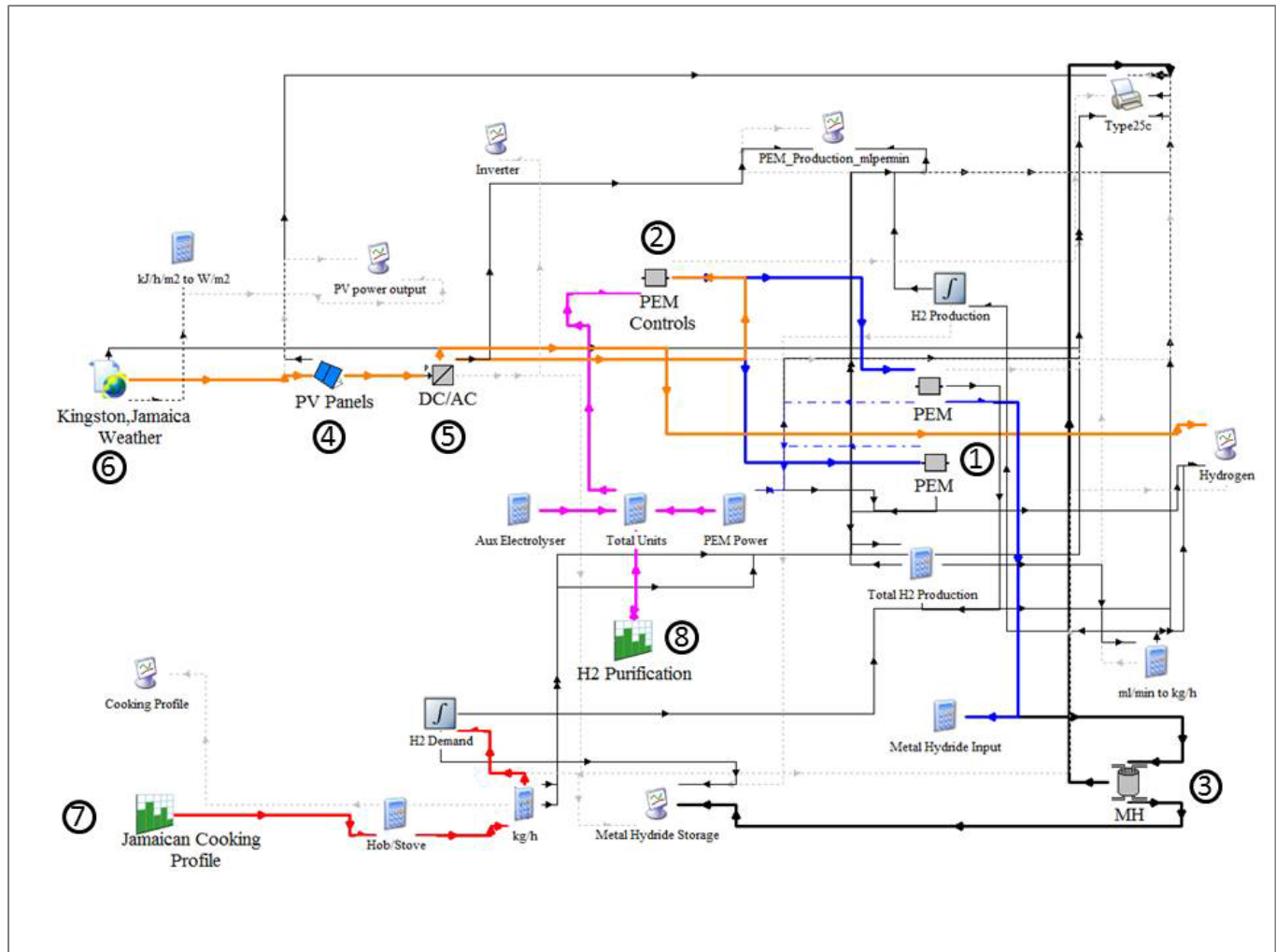


**Figure 1: Screenshot of the developed model for the case study application. The model’s main parts consist of the PV array (4) that supplies the PEM electrolyser (1) through an inverter (5), the electrolyser auxiliary components (controls (2), and gas management parts (8)), and the metal hydride storage components (3). It also includes the necessary weather data (6) for the simulation, the cooking load profile for the application (7) and other computational components. The electrolyser is supplied through the PV, according to their yield which depends on the weather data.**

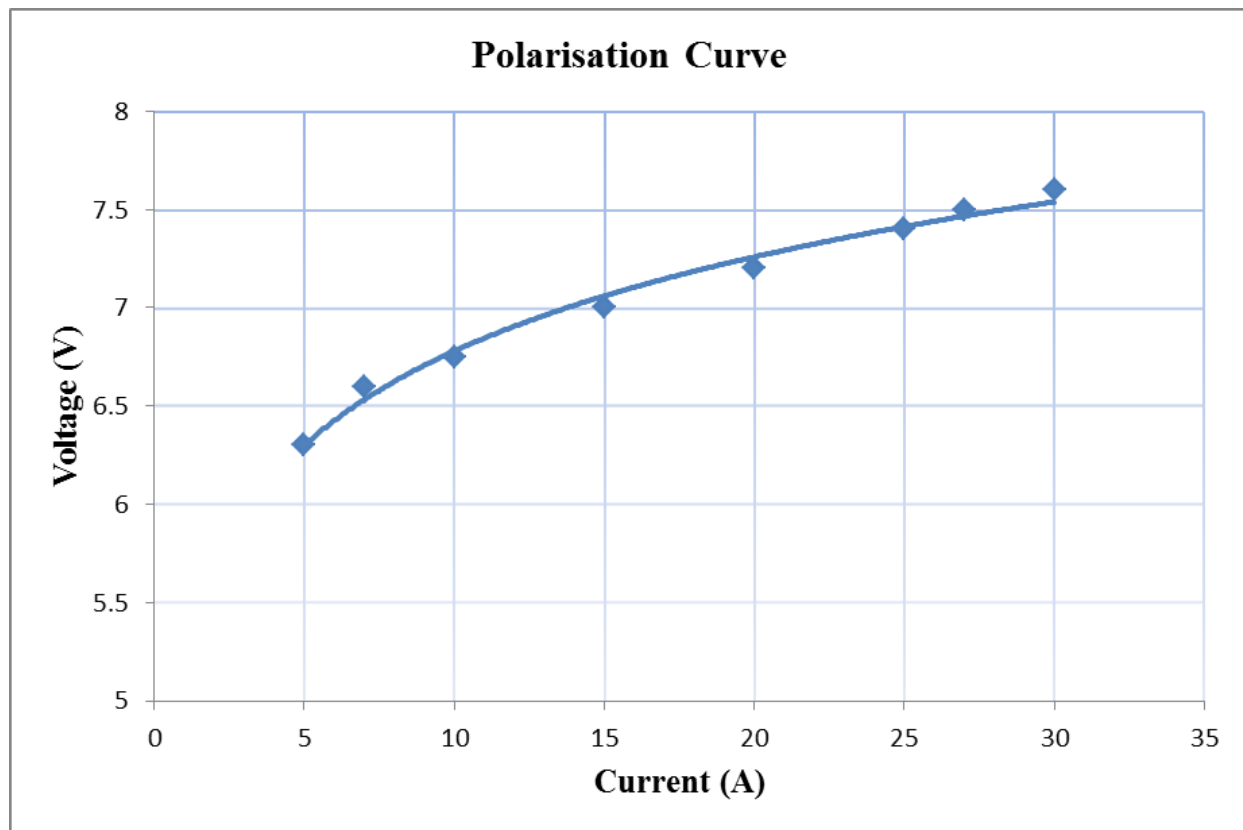


Figure 2: Electrolyser stack I-V curve

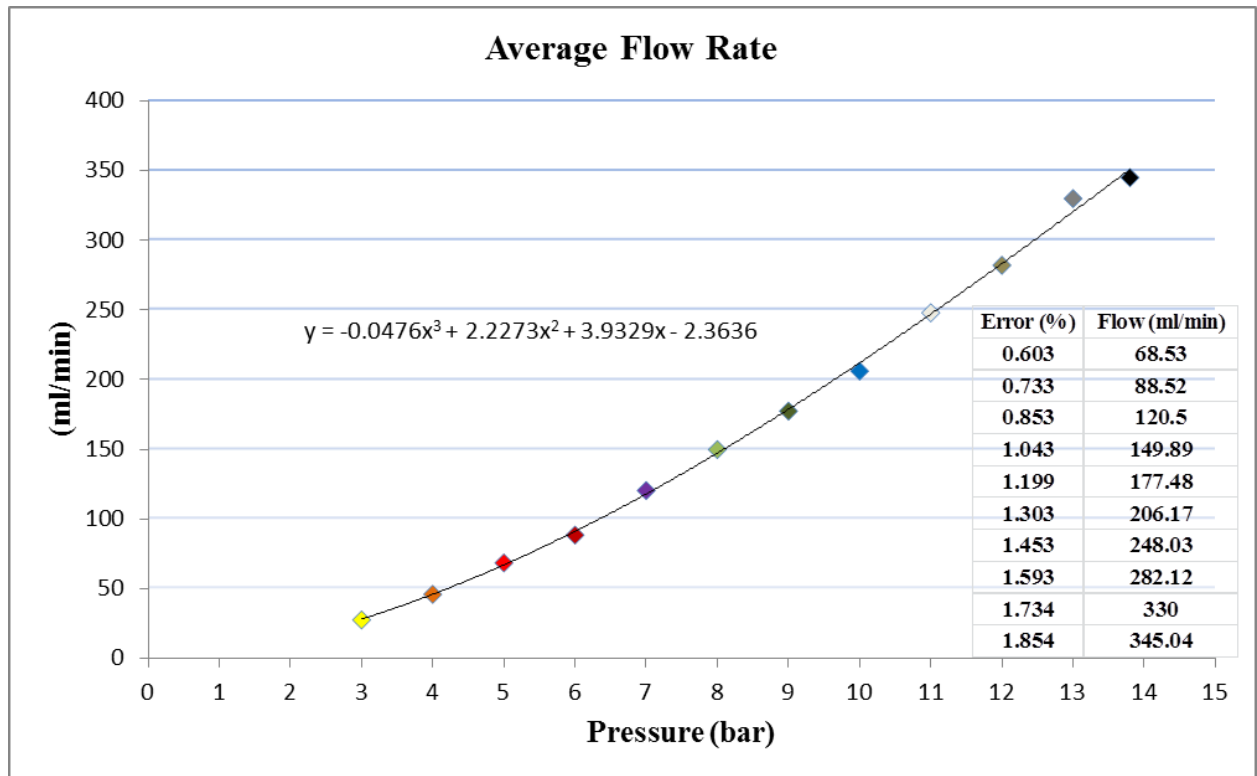


Figure 3: Average hydrogen flow rates curve for the complete pressure range of the electrolyser, 3 to 13.8bar

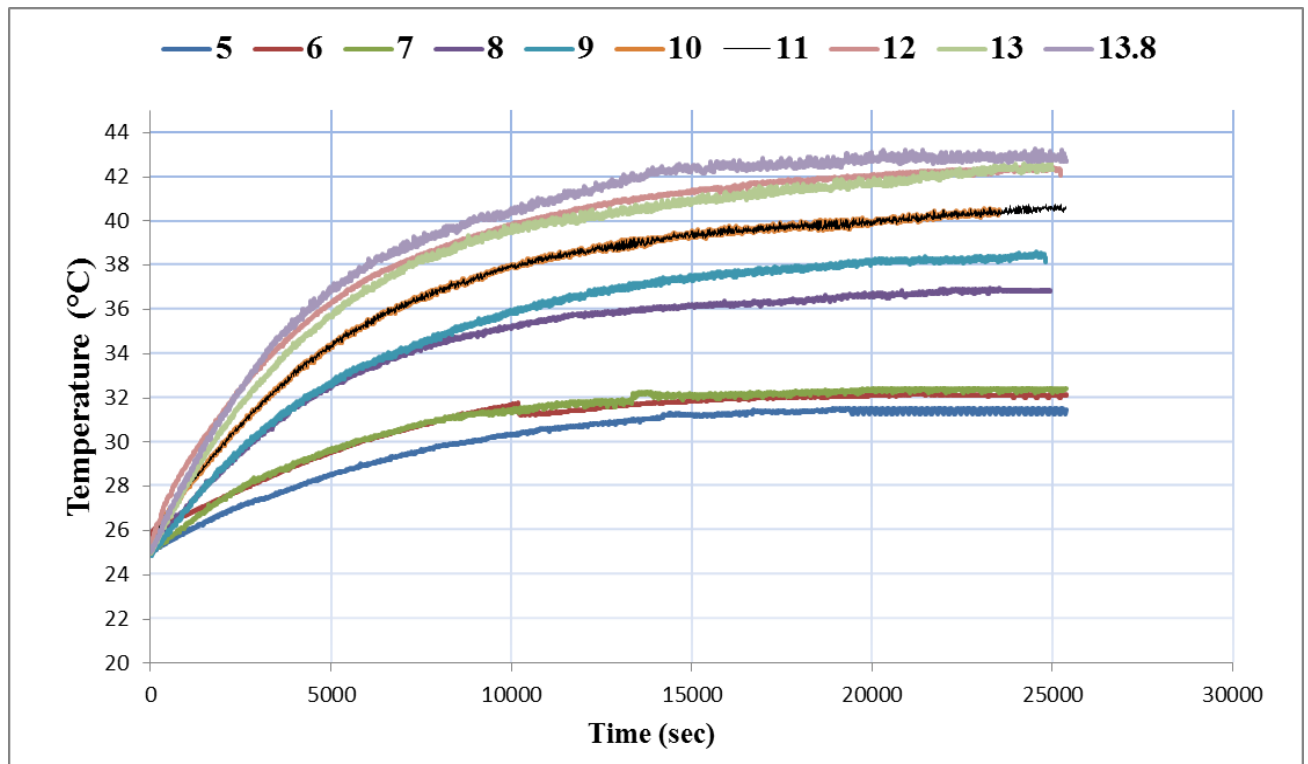


Figure 4: Experimental temperature measurements for pressures of 5 to 13.8 bar

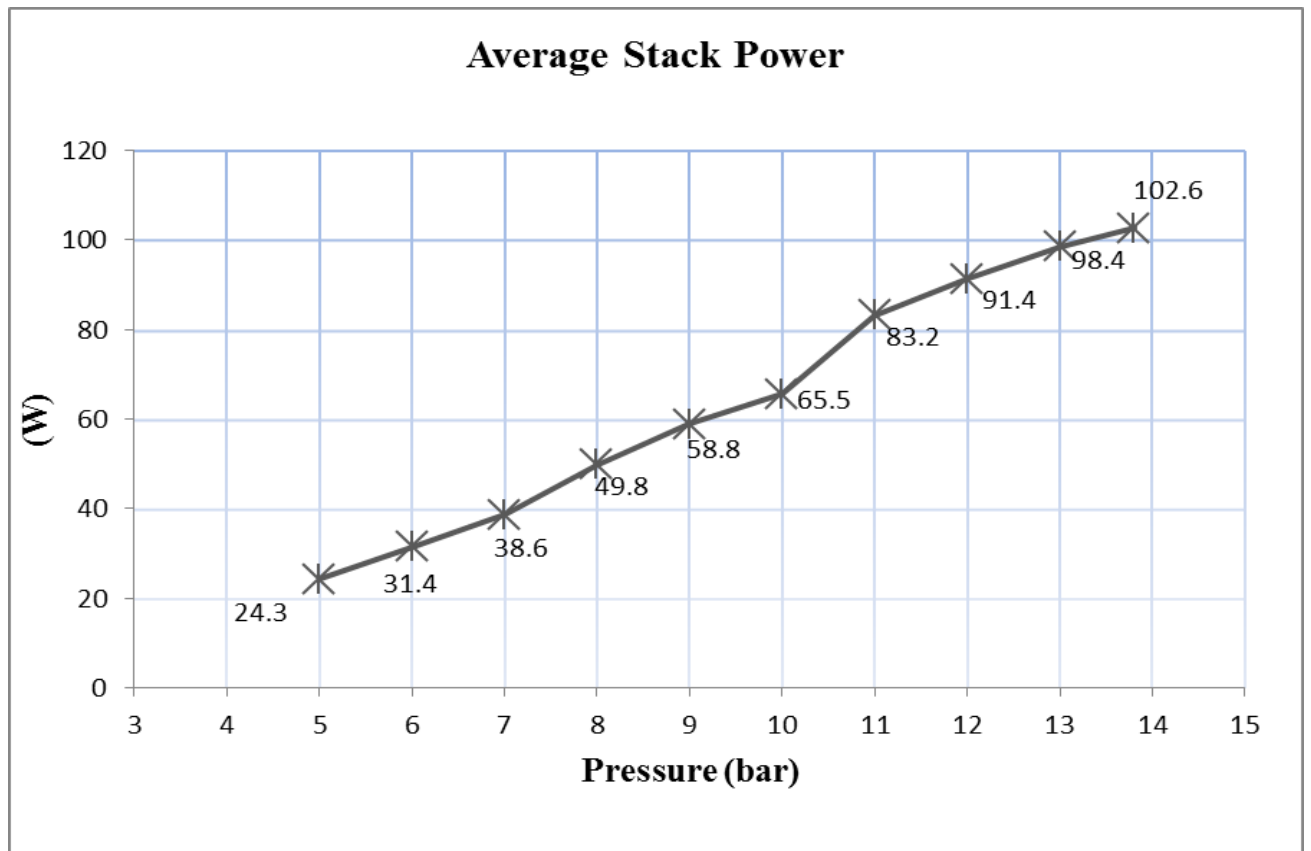


Figure 5: Experimentally measured energy use of the stack for pressures of 5 to 13.8 bar

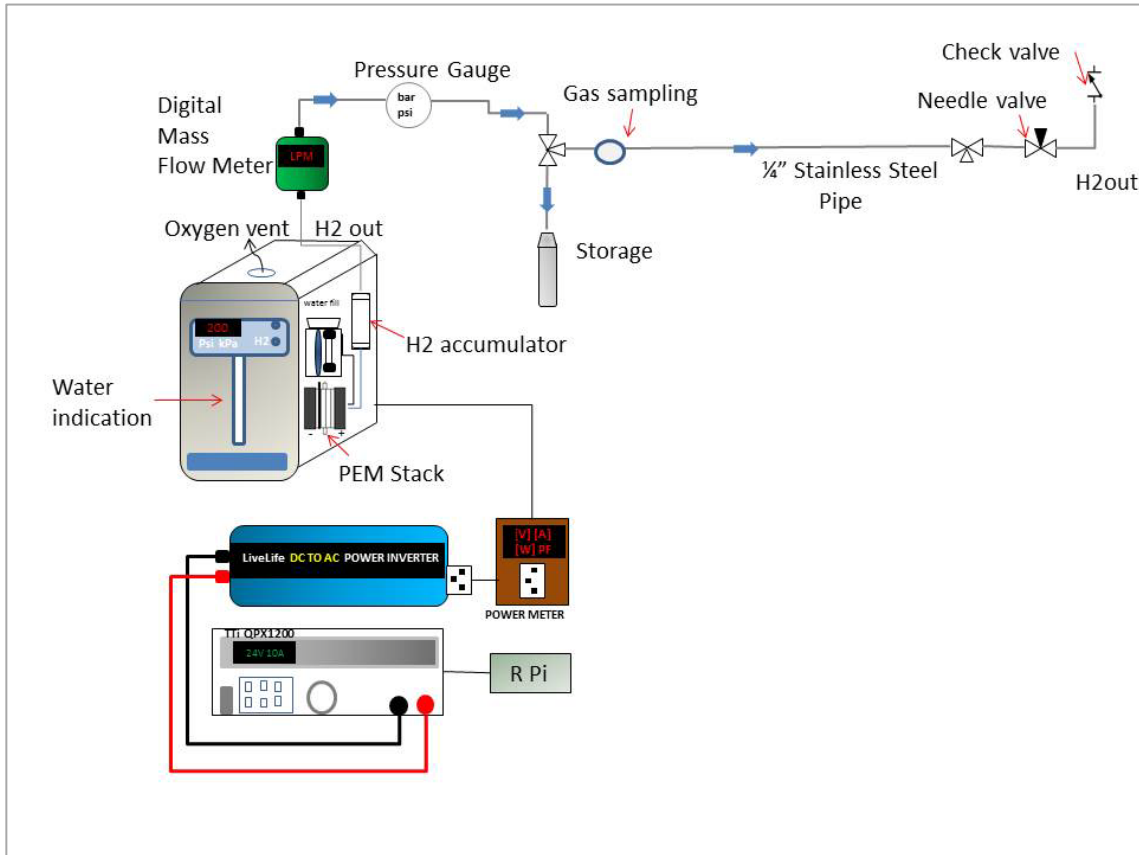


Figure 6: Experimental Setup Design

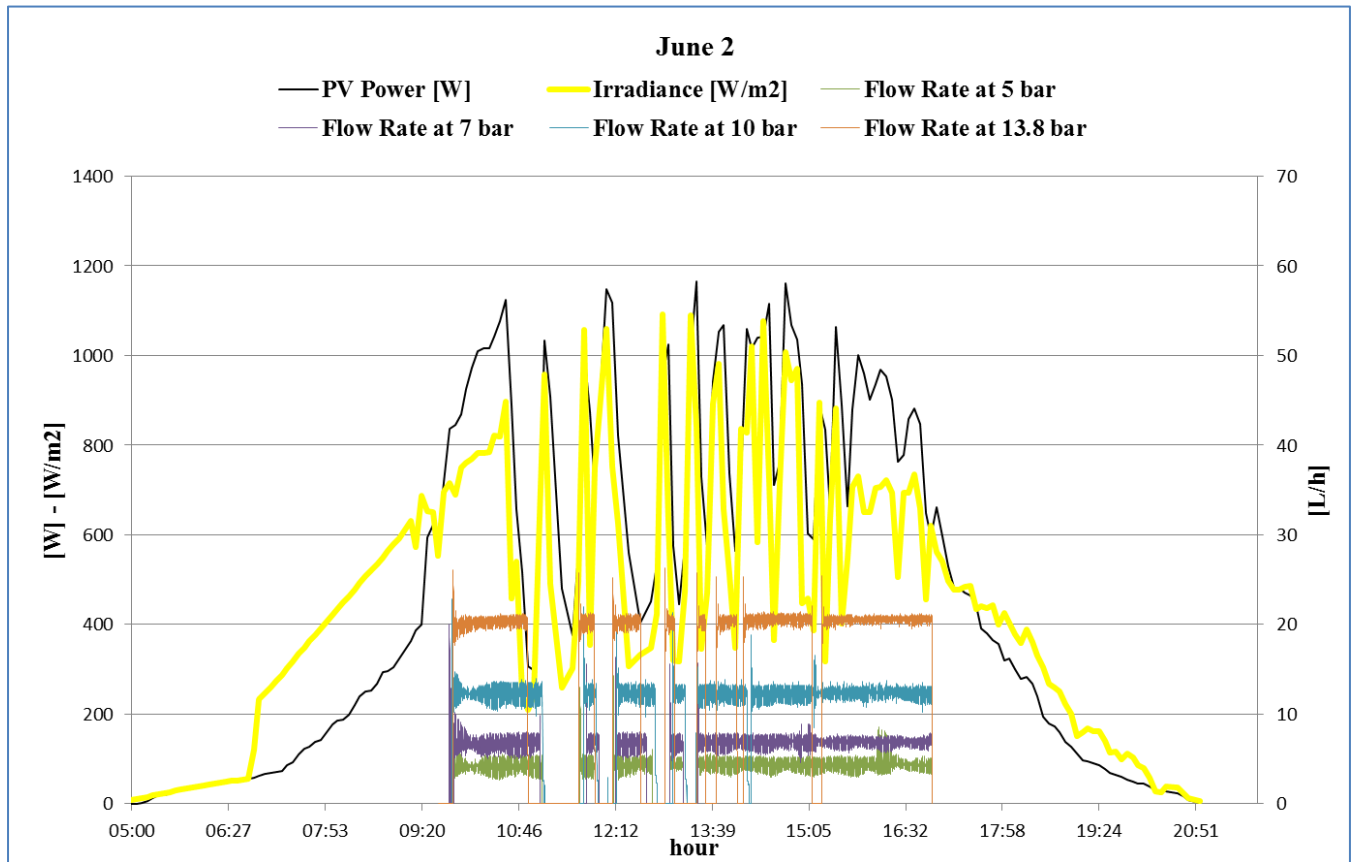


Figure 7: Hydrogen production rate in L/h at different pressure set points during June 2<sup>nd</sup> that presents unstable irradiance levels

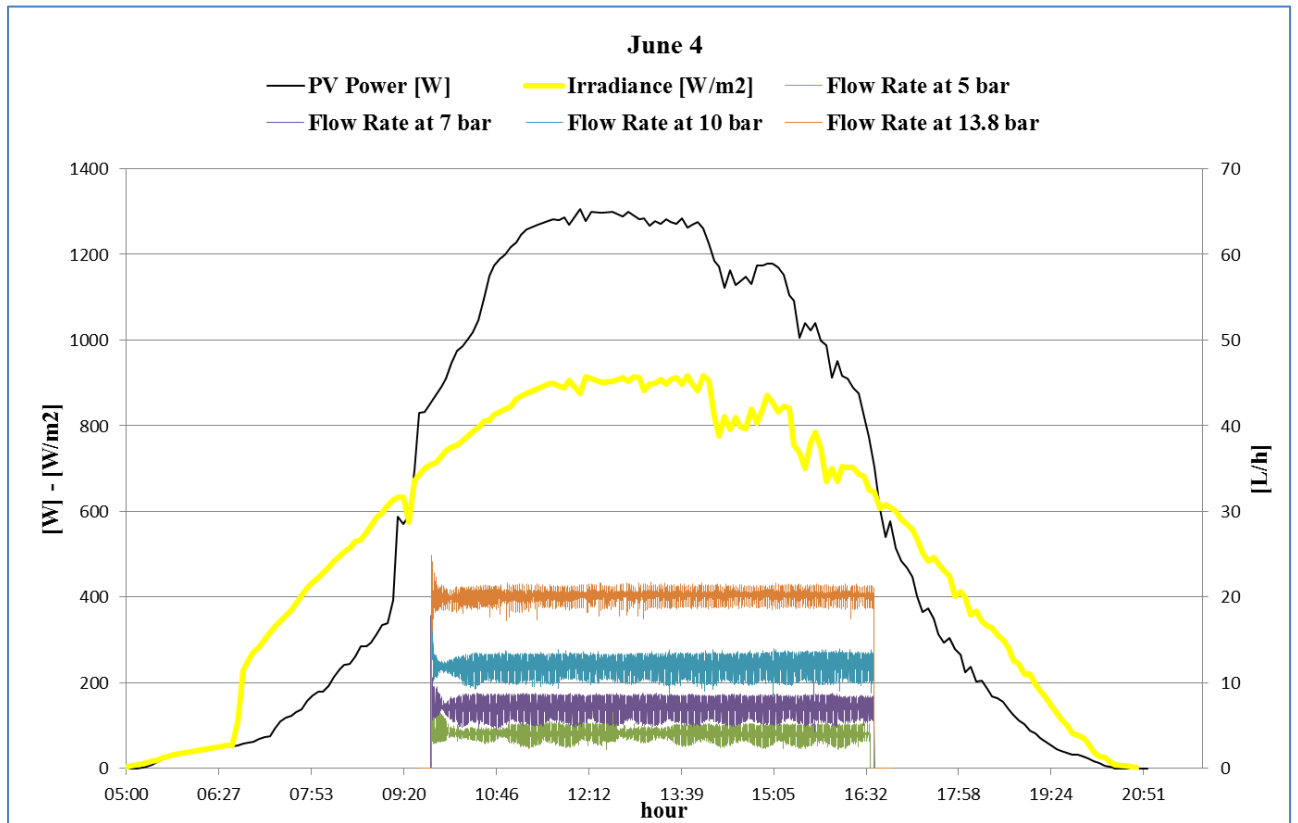


Figure 8: Hydrogen production rate in L/h at different pressure set points during June 4<sup>th</sup> that has consistently high irradiance level

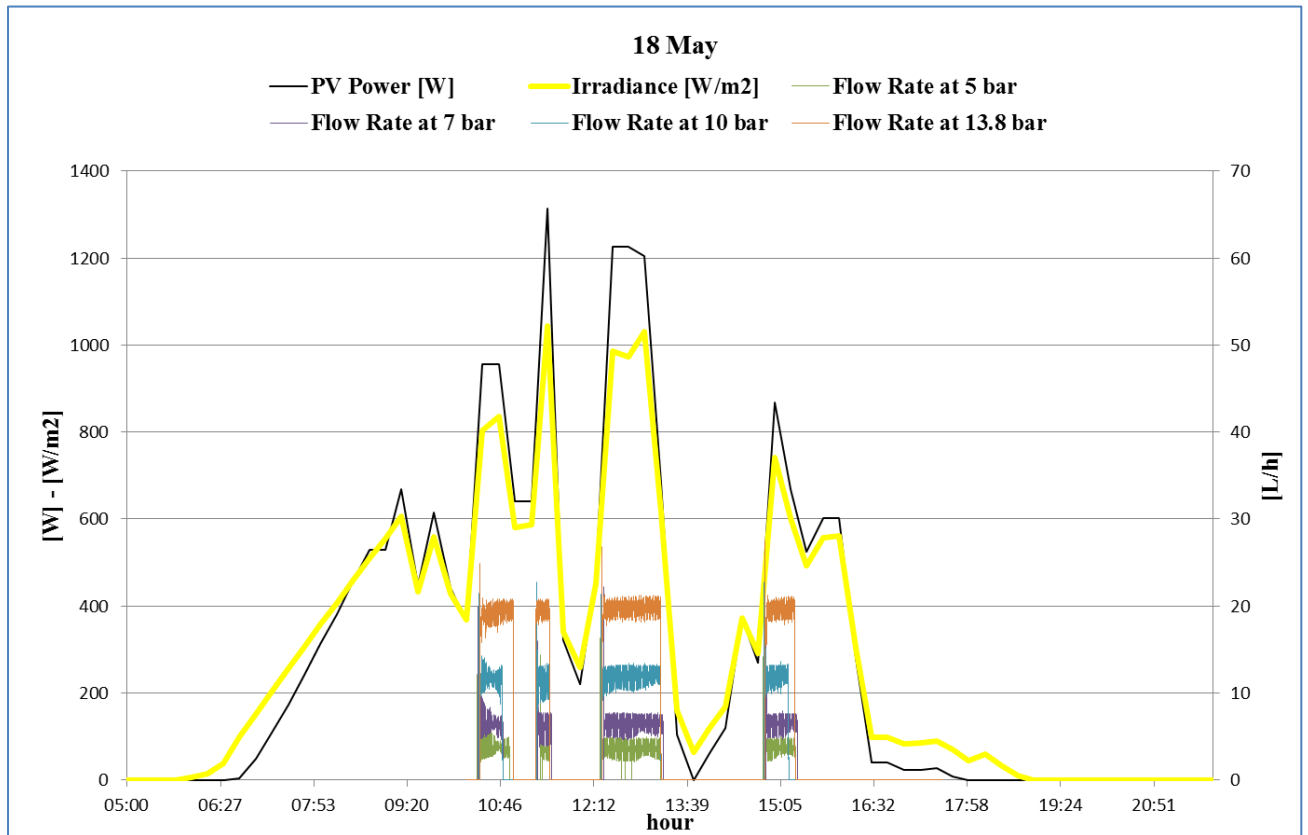


Figure 9: Hydrogen production rate in L/h at different pressure set points during May18th that presents unstable irradiance levels for the high irradiance period

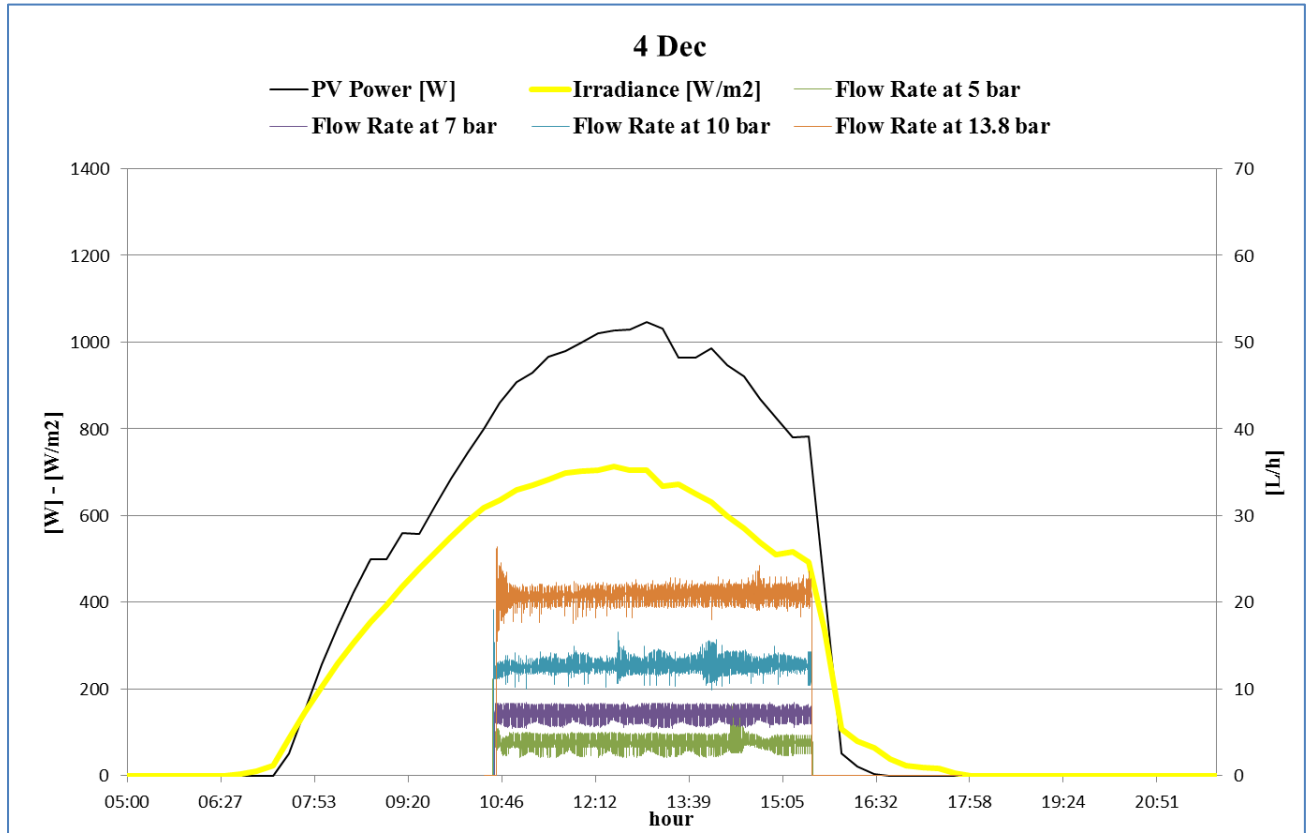


Figure 10: Hydrogen production rate in L/h at different pressure set points during December 4th that has consistently high irradiance levels for the low irradiance period

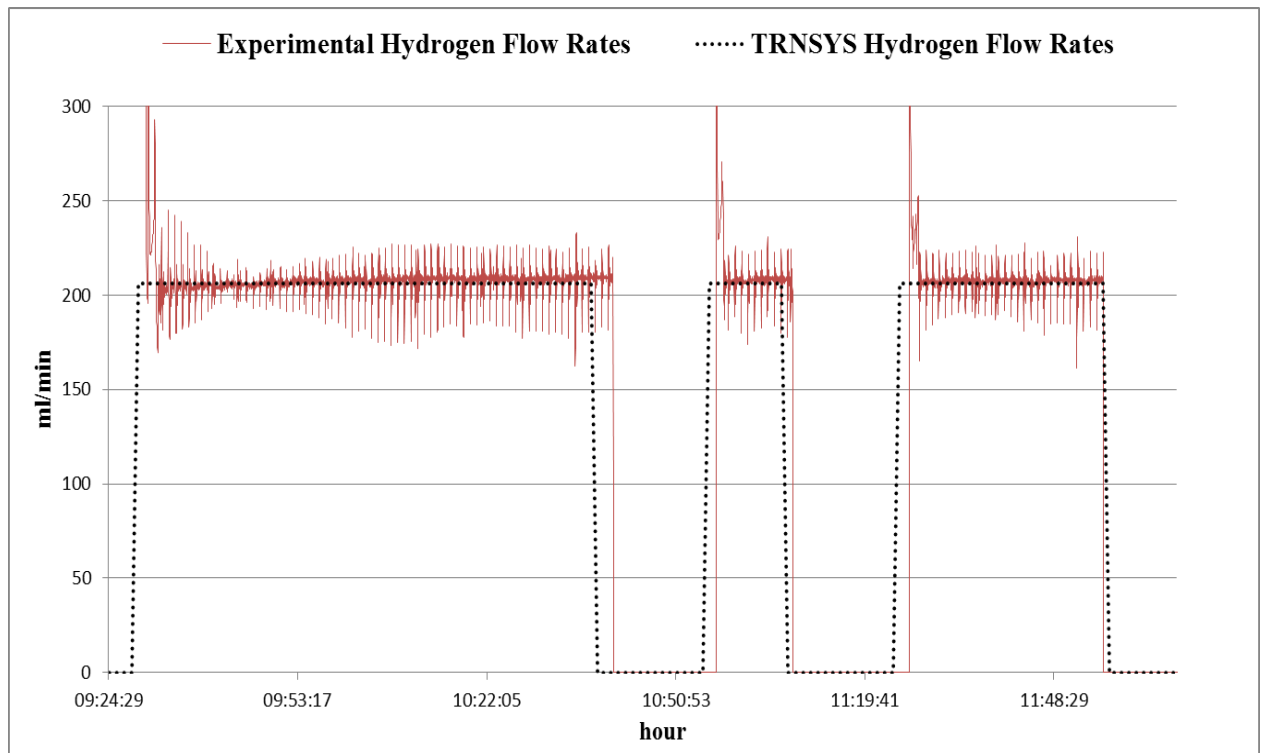


Figure 11: Comparison between TRNSYS and experimental results of produced hydrogen flow rates

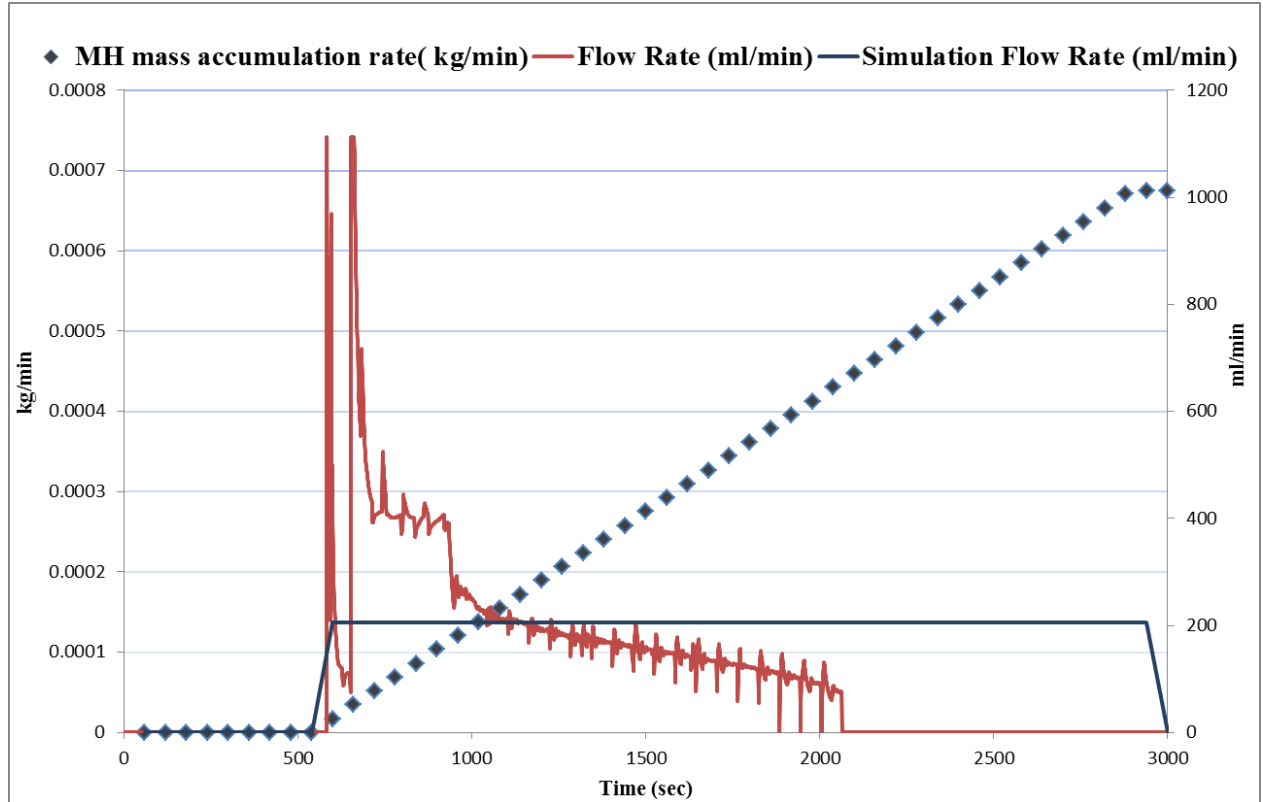


Figure 12: Comparison between experimental and simulation results for the metal hydride tank absorption process

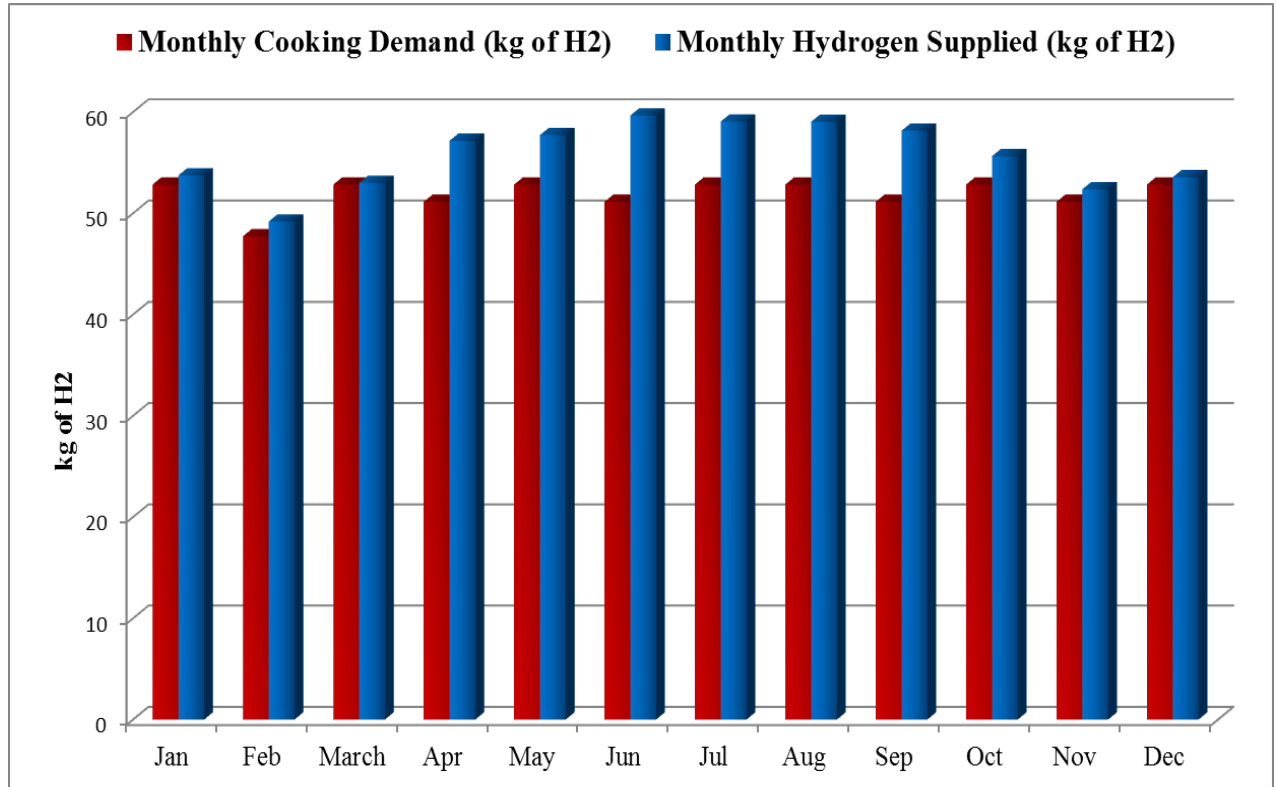


Figure 13: Monthly hydrogen production and demand

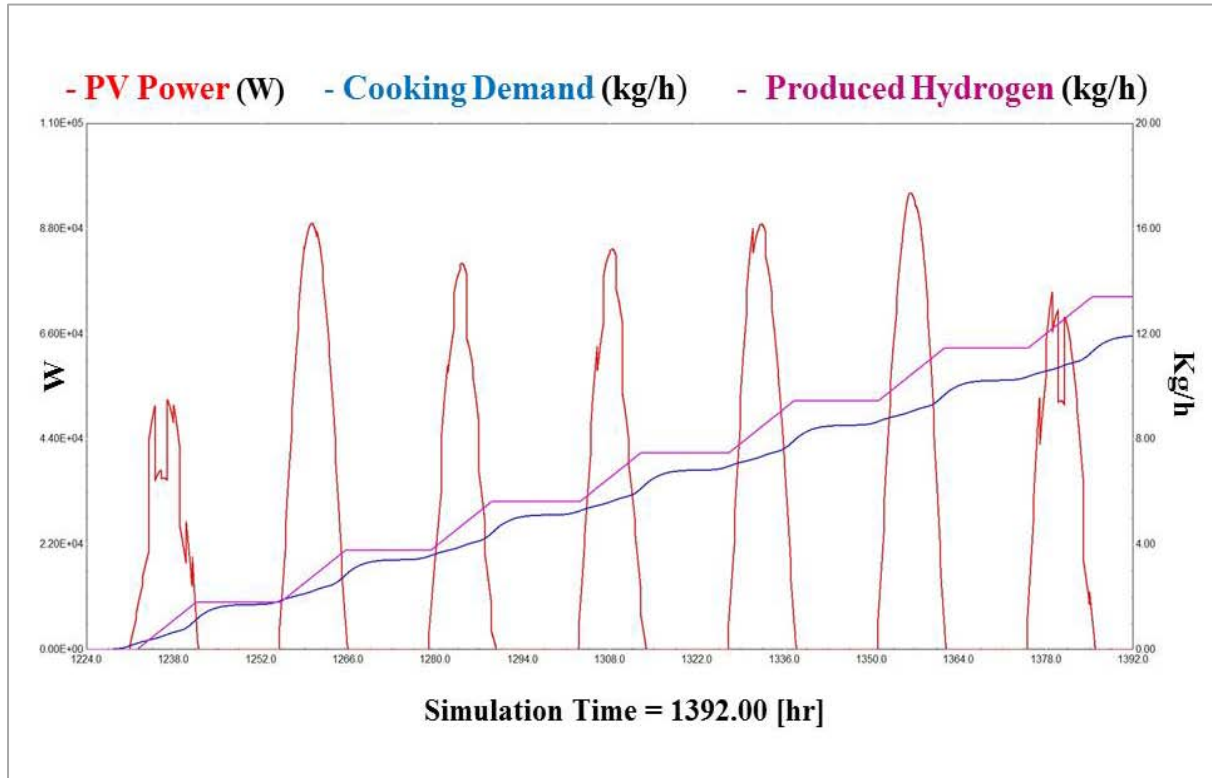


Figure 14: TRNSYS simulation results regarding PV power, accumulated hydrogen production rates and cooking demand for a week in February

**Table 1, Semi and total reaction in the Proton Exchange Membrane electrolytic cell**

Anode	$H_2O \rightarrow \frac{1}{2}O_{2(g)} + 2H^+ + 2e^-$
Cathode	$2H^+ + 2e^- \rightarrow H_{2(g)}$
Total	$H_2O \rightarrow H_{2(g)} + \frac{1}{2}O_{2(g)}$

**Table 2, Coefficient of performance of the PEM electrolyser operation**

Pressure Set Point (bar)	Operation Coefficient
3	0.034
4	0.055
5	0.080
6	0.110
7	0.140
8	0.172
9	0.208
10	0.246
11	0.286
12	0.326
13	0.370
13.8	0.403

**Table 3, Electrical and Thermal characteristics of the PV modules of the experimental PV emulator**

PV Type	Sanyo Heterojunction with Intrinsic Thin Layer (HIP)- 210NHE1	Sharp MonoSi NUS5E3E/NU185E1	TrinaSolar TSM- 180DA01
Nominal Power Output $P_{MP}$	210	185	180
$V_{MP}$ [V]	41.3	24	36.8
$I_{MP}$ [A]	5.09	7.71	4.9
$V_{OC}$ [V]	50.9	30.2	44.2
$I_{SC}$ [A]	5.57	8.54	5.35
Temperature Coefficient of Power [%/°C]	-0.30	-0.485	-0.45

**Table 4, Experimental results on the energy use, hydrogen production and energy efficiency at different operation conditions**

Pressure Set-point (bar)	Average Flow Rate (ml/min)	Max Temperature (°C)	Stack Efficiency (%) For constant operation		Stack Efficiency (%) For variable power input operation		kWh/Nm <sup>3</sup> For constant operation		kWh/Nm <sup>3</sup> For variable power input operation	
			June 4 <sup>th</sup>	Dec 4 <sup>th</sup>	June 2 <sup>nd</sup>	May 18 <sup>th</sup>	June 4 <sup>th</sup>	Dec 4 <sup>th</sup>	June 2 <sup>nd</sup>	May 18 <sup>th</sup>
			5	68.53	31.56	43.57	39.37	37.02	36.68	7.50
7	120.50	32.45	57.0	55.97	53.5	40.86	5.73	5.84	6.10	7.99
10	206.17	37.18	57.23	56.98	52.9	40.59	5.71	5.74	6.17	8.05
13.8	345.04	43.25	63.64	60.93	56.16	47.37	5.14	5.36	5.82	6.89

**Table 5, Total generated hydrogen for the representative experimental days**

Pressure Set-point (bar)	June 2 <sup>nd</sup>	June 4 <sup>th</sup>	May 18 <sup>th</sup>	Dec 4 <sup>th</sup>
5	25.6	27.55	8.51	18.98
7	42.9	47.31	13.84	33.50
10	77.71	84.41	23.11	61.49
13.8	118.5	137	51.75	101.49